19, 533 (1965).
[44]A. D. B. Woods and R. A. Cowley, Phys. Rev. Letters 24, 646 (1970).
[45]D. Pines and C. W. Woo, Phys. Rev. Letters 24, 1044 (1970).
[46]S. Eckstein and B. B. Varga, Phys. Rev. Letters 21, 1311 (1968).
[47]S. Sunakawa, S. Yamasaki, and T. Kebukawa, Progr. Theoret. Phys. (Kyoto) 41, 919 (1969); T. Kebukawa, S. Yamasaki, and S. Sunakawa, *ibid.* 44, 565 (1970).

PHYSICAL REVIEW A VOLUME 5, NUMBER 3 MARCH 1972

Spectroscopic Study of the Early Afterglow of a Recombining Helium Plasma

J. Stevefelt*
AB Atomenergi, Studsvik, Fack, S-61101 *Nyköping, Sweden*

and

F. Robben†
Department of Mechanical Engineering, University of California, Berkeley, California 94720

(Received 14 June 1971)

The afterglow of a 1.3-A 1.5-μsec-duration discharge in helium at 11 Torr was studied in some detail during the times 15 to 35 μsec after the discharge pulse. Spectroscopic measurements were used to obtain the number densities of excited atomic and molecular states, the conductance of the plasma column was determined from simultaneous electric field and current measurements, and a 10-μsec current pulse was used to selectively heat the electrons, thus disturbing some of the afterglow processes. The atomic and molecular ion densities and the electron temperature, obtained from the spectroscopic measurements, were in good agreement with the plasma conductance and field strengths. The inferred recombination rate favors the recent calculations of Mansbach and Keck over the Bates, Kingston, and McWhirter calculations of the collisional radiative-recombination rate. The rate of conversion of atomic into molecular ions was dominated by associative ionization of excited atomic states, and good agreement was obtained by including this process with other known processes.

I. INTRODUCTION

The decaying afterglow of electrical discharges in helium has been the subject of a very large number of experimental and theoretical investigations. In the last ten years we have collected almost 100 published papers dealing either directly with the helium afterglow or with processes which are of particular importance. Although the level of understanding has certainly increased as a result of all this labor and speculation, it is disconcerting to realize how much is still unknown.

For low-pressure afterglows ($p < 0.1$ Torr) the so-called collisional radiative-recombination model[1–3] is now generally considered to be a correct representation,[3–17] and only the rate constants in this model, and the finer details of the fate of the principal-quantum-number-two atomic states, intimately connected with the electron energy balance, need further clarification. For medium-pressure afterglows ($0.1 < p < 100$ Torr), where the molecular helium ion becomes important, an appropriate model which completely encompasses the observed phenomena has yet to be found.[8,18–28] However, a number of the experimental observations of afterglows in this pressure range have been explained reasonably satisfactorily. For high-pressure afterglows ($p > 100$ Torr) there have so far been only a few experimental measurements,[29–31] which indicate a very complex situation that is only beginning to be understood. Some preliminary measurements on pulsed and steady-state low-current arcs at near atmospheric pressure, where the molecular ion concentration is small, also showed unexplained phenomena.[32]

One concludes that useful experiments are very difficult to perform, and that as a corollary there are numerous errors in the published papers. A good review of the situation would be invaluable as an aid in determining what future work should be the most useful, and with what degree of care measurements must be performed. Such a review would be a quite difficult undertaking which is not attempted in the present paper; we have only cited some representative references to accompany the preceding brief comments.

The work presented in this and the following paper was initiated as a result of a proposed type of magnetohydrodynamic generator which would use an auxiliary ionization source to partially ionize the helium working gas, and would depend on a relatively slow recombination rate to maintain a reasonable electrical conductivity in the generator channel.[33,34] Thus a study of the recombination mechanisms and

rates in high-neutral-pressure low-ionization-degree helium plasmas was begun. The principal diagnostic method chosen was time- and space-resolved spectroscopic measurements of the absolute intensity of a pulsed helium afterglow, accompanied by probe measurements of the plasma column conductivity. Like several other experimenters, we have used the phenomenon of afterglow quenching[35,36] and its influence upon the light emission and the conductivity is studied. In an attempt to gain confidence in the diagnostic methods, initial measurements were made at a pressure of 11 Torr, where it was thought that existing models could satisfactorily describe the experimental results. This was not true, however, and in the following paper a new process is proposed in order to explain some of our results. In general, the diagnostic methods used here are inadequate for the task of completely unravelling the complex processes involved in higher-pressure helium afterglows.

In this paper measurements of the atomic and molecular ion densities, the electron temperature, and the plasma column conductance are described in the early afterglow. The conservation equations for electron density, ion species density, and electron energy are checked using known processes and rate coefficients, and in general reasonable agreement is found within a rather large experimental error. The measured and calculated plasma column conductances were also checked in detail. It was inferred from the measurements that the process of associative ionization and its inverse, dissociative recombination, were not properly understood, and the measurements pertaining to this process are described in the following paper, where a new model is proposed.

II. EXPERIMENTAL EQUIPMENT

A block diagram is shown in Fig. 1. The discharge was created in a 7.7-mm-diameter glass tube, 40 mm long, between a thermionically emitting tungsten cathode and a plate anode. This tube had a 3-mm gap in the middle so that spectroscopic observations could be made without distortion by the glass tube, and the whole arrangement was enclosed in a stainless-steel chamber with Viton O-ring seals. Helium, purified by passing through a quartz leak, flowed continually through the chamber. Impurities outgassing from the O rings were unimportant for the measurements described here, but became important at higher pressures, where they precluded measurements.

The discharge was pulsed at 100 Hz, had a maximum current of 1.3 A, and was 1.5 μsec long. All experiments were performed at a helium pressure of 11 Torr. The heating of the gas by the discharge pulse was negligible, and the gas temperature was measured to be approximately 450 °K

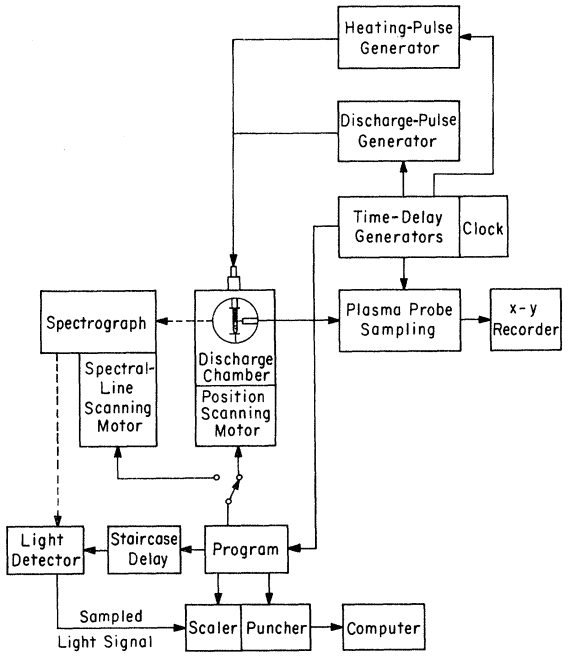

FIG. 1. Block diagram of the electronic control and data recording for the pulsed discharge.

with a tungsten-wire resistance thermometer.

The light emitted from a small region of the plasma column is focussed by a system of mirrors on the entrance slit of a 1-m grating spectrometer. At the exit slit single photoelectrons from a 1P28 photomultiplier are counted on a scaler for a preset number of discharge cycles and recorded on punched paper tape. By using a tungsten-ribbon filament lamp, calibrated for brightness, the spectrometer-photomultiplier combination was calibrated for absolute intensity measurements.

The photoelectron counting system was gated on at a preset delay time after each discharge, and stayed on for a preset gate time, so that synchronously sampled light detection was achieved. The discharge chamber could be automatically moved in steps by a motor, so that the true radial distribution of light intensity could be obtained by means of an inversion, which was performed by using the numerical method described by Bockasten.[37]

Two floating probes inserted into the plasma column 20 mm apart were used to determine the electric field strength when a small pulse of current was passed through the decaying plasma, and thus the plasma conductance was measured. Larger pulses of current were used to heat selectively the electrons. Further description of the experiment and some preliminary analysis is given in the report by Stevefelt.[38]

III. AFTERGLOW PROCESSES

It has been shown that three-body electron-elec-

tron-ion recombination into highly excited levels, followed by electron collisional and radiative cascading to the ground state, is the dominant ion loss process under a wide variety of conditions in helium plasmas.[1-28] This process, termed collisional radiative recombination by Bates, Kingston, and McWhirter,[1] can be represented by the following reactions:

$$\begin{aligned} &He^+ + 2e^- \leftrightarrows He^{(n)} + e^- , \\ &He^{(n)} + e^- \leftrightarrows He^{(m)} + e^- , \\ &He^{(n)} \rightarrow He^{(m)} + h\nu . \end{aligned} \tag{1}$$

These processes produce excited-state densities which are predictable functions of the electron temperature and density, and thus the presence of collisional radiative recombination can be verified by quantitative spectroscopic measurements. This process is expected to be applicable to molecular helium ions as well as to atomic ions,[19,39] although there are definitely other complications which affect the molecular ions.[27,28]

Dissociative recombination had at one time been thought responsible for the rapid recombination rate measured in early microwave studies of the helium afterglow.[40] This process is the inverse of associative ionization,

$$He^{(n)} + He \leftrightarrows He_2^+ (v) + e^- , \tag{2}$$

discussed in the next paragraph. The vibrational state v of the molecular ion must be the ground state if molecular ions at room temperature are to participate. Spectroscopic studies have shown quite conclusively that dissociative recombination from the ground vibrational state does not occur to a significant extent,[8,19] and Mulliken[39] has stated that this is reasonable in view of the expected behavior of the potential energy curves of excited He_2.

Associative ionization, process (2), is responsible for creating molecular helium ions from excited atomic states, and was originally found in mass spectrometer studies.[41] It was later determined[42] that the excited atomic state must have a principal quantum number of at least 3 in order that process (2) be energetically possible.[43] The associative ionization rate constant has been determined for some $n = 3$ atomic states by Teter, Niles, and Robertson.[44]

Atomic ions are directly converted into molecular ions by a three-body process,

$$He^+ + 2He \rightarrow He_2^+ + He , \tag{3}$$

whose rate constant has been determined by several experimenters.[8,45-48] Paired collisions of metastable He (2^3S) atoms result in atomic ions,

$$He(2^3S) + He(2^3S) \rightarrow He^+ + He + e^- , \tag{4}$$

a process whose rate constant has also been determined by several experimenters.[49-53] The formation of excited molecular helium from excited atomic helium by a three-body process is negligible, if the rate is not larger than that measured by Teter and Robertson[54] for $He(2^3P)$.

The deexcitation of the metastable $He(2^3S)$ state by electron collisions,

$$He(2^3S) + e^- \rightarrow He(1^1S) + e^- + 19.8 \text{ eV} , \tag{5}$$

is important in the electron energy balance. The rate constant has been calculated from the excitation measurements of Schulz and Fox[55] by Bates, Bell, and Kingston,[52] and is approximately constant in the range $1000 < T_e < 4000\ ^\circ\text{K}$. Gryzinski's 1959 semiclassical prescription[56] gives a rate constant about 80% larger, while his later results[57] for optically forbidden transitions lead to a much smaller rate constant which is only about 26% of that given by Bates *et al.* Poukey, Gerardo, and Gusinow,[58] using the excitation cross-section calculations of Morrison and Rudge,[59] find a rate constant proportional to $T_e^{1/2}$ which is about one-third the value of Bates *et al.* in the above-quoted temperature range.

It has been shown by Ingraham and Brown[60] that the inverse of process (5) cannot be generally neglected, and they give a result applicable to the case where process (5) is in approximate equilibrium and the net rate is determined by electron-electron collisions. As discussed in Sec. IV E, their model predicts a moderate decrease in the rate of process (5) for the conditions of the present experiment.

Finally, the ambipolar diffusion coefficient of the atomic and molecular ions has been measured by many experimenters, with good agreement among the more recent determinations.[8,61]

IV. EXPERIMENTAL RESULTS

A. Late Afterglow Decay

For delay times greater than 300 μsec both the helium atomic lines and the helium molecular bands decay with a characteristic rate of approximately -1.2×10^4 sec^{-1}. This is in agreement with the experiments and analysis of Gerber, Sauter, and Oskam[8] for the case where ambipolar diffusion dominates the electron loss, in combination with three-body formation of molecular ions, process (3), and collisional radiative recombination as the source of light for both the atomic lines and molecular bands. Under these conditions the characteristic rate for electron loss is approximately one-third of that for the radiation, due to the three-body nature of process (1).[62] This is also in agreement with the time constant of our measured values of plasma conductance, which is proportional to the electron density in the late afterglow.

Some weak impurities were found in the emitted spectrum, which have been identified as nitrogen

and hydrogen. The N_2^+ band at 3914 Å decayed much slower than the helium lines and bands; for delay times greater than 300 μsec it decayed exponentially with a characteristic rate of -4×10^3 sec^{-1}. During the first 200 μsec of the afterglow the nitrogen band intensity was much brighter some distance outside the discharge than it was at the center, while in the late afterglow the radial variation of intensity was similar to that for helium. Since the N_2^+ band is probably formed by a Penning process from the ground state, it is possible that virtually all of the nitrogen is ionized in the center of the column during the early afterglow, resulting in a decrease in the rate of the Penning process. This assumes that a Penning process is not able to excite the N_2^+ band from the ground N_2^+ state.

It is not clear if the N_2^+ band is excited by the metastable He($2\,^3S$) atoms or by helium ions. Later measurements of the He($2\,^3S$) decay gave a characteristic rate of -1.5×10^3 sec^{-1}, while the characteristic decay rate of -3.8×10^3 sec^{-1} found for the electron (and ion) density in the later afterglow agrees well with that found for the N_2^+ band. The impurity content, however, was less in the later He($2\,^3S$) measurements, which could play a significant role.

The hydrogen Balmer series rose in intensity in the early afterglow, and later decayed with a characteristic rate of -7.1×10^3 sec^{-1}. The radial distribution was similar to helium. These lines were strongly quenched in the afterglow when the electron temperature was raised, indicating that they result from recombination of hydrogen ions. The nitrogen bands were not quenched at all by electron heating, as expected for a Penning excitation process.

This impurity radiation was less than 1% of the intensity of the strongest rotational line of He_2 in the early afterglow, and thus should not affect the measurements. Subsequent experiments in which the purity was significantly increased showed no effect in the early afterglow. However, in the late afterglow (especially at higher helium pressures) the impurity content definitely affected the results and precluded measurements with the present system.

In addition to numerous very weak, unidentified lines (probably molecular helium), there appeared to be a continuous weak background radiation throughout the visible spectrum, which decayed with time.

B. Electron Temperature and Density from 15- to 35-μsec Delay

The logarithm of the number density of the excited states of atomic helium on the center line of the plasma column ($r=0$) plotted versus ionization energy is shown in Figs. 2 and 3 for 20- and 35-μsec delay. By assuming equilibrium between the highly excited states and the free electrons,

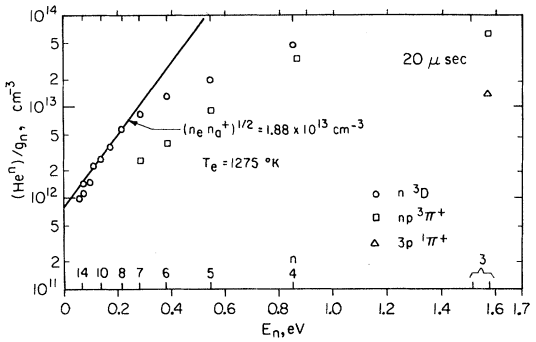

FIG. 2. Plot of the logarithm of the excited helium state densities versus the ionization energy of the state, on the axis of the plasma column at 20-μsec delay after the end of the discharge pulse.

given by the Saha equation,

$$n_e n_i/n_u = (g_e g_i/g_u)(2\pi m_e kT_e/h^2)^{3/2}\, e^{-E_u/kT_e}, \quad (6)$$

the product of ion and electron density and the electron temperature can be found. In Eq. (6), n_u is the excited-state density, E_u is the ionization energy of this state, the g's are the multiplicities of the states, and the other symbols have their usual meaning. From these and other plots it is found that the electron temperature is approximately constant, both in time from 15- to 35-μsec delay and in space with radial position.

In Fig. 3 the relative populations of lower states with the same principal quantum number indicate a "population temperature" equal to the electron temperature, with the exception of the ^3S state, as was previously found by Robben *et al.*[4] under somewhat different conditions. This indicates that the electron-induced collision rates between these states is considerably larger than the net radiative rates.

Some excited-state molecular densities are also shown in Fig. 2, obtained from measurement of the total molecular band intensities. The oscillator strengths for these bands, given in the Appendix, were calculated by use of the Coulomb approximation as given by Bates and Damgaard.[63] For large principal quantum numbers where Saha equilibrium with the electrons is approached, the molecular densities are about 30% of the atomic densities, which gives a molecular ion density 30% of the atomic ion density.

The characteristic decay rate of the atomic lines with large principal quantum number was found to be -2.8×10^4 sec^{-1}, while the characteristic decay rate of the corresponding molecular bands was equal to zero, within the experimental error, at a delay time of 25 μsec. From this, the fraction of molecules at 20-μsec delay, and the value of $n_e n_i$ given in Fig. 3 at 35 μsec, we find the atomic and molecular ion and the electron densities during the pe-

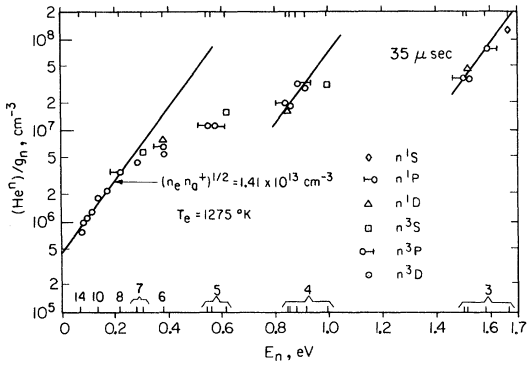

FIG. 3. Excited helium state densities on the axis of the plasma column at 35-μsec delay.

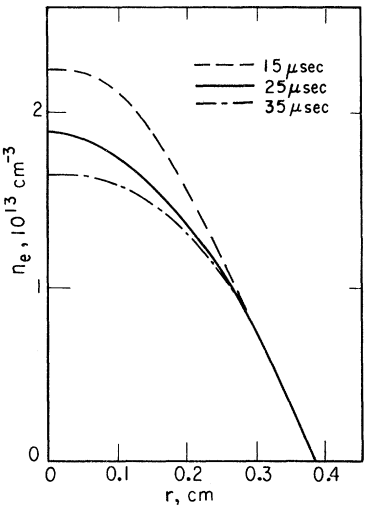

FIG. 5. Variation of the electron density with radius in the plasma column, at three different delay times.

riod 15–35 μsec shown in Fig. 4. The atomic ion density is decaying during this period while the molecular ion density is increasing.

The variation of electron density with radial position in the plasma column was also calculated from the spectroscopic measurements, and is shown in Fig. 5 at 15-, 25-, and 35-μsec delay. These measurements were extrapolated to zero at 3.85 mm, the tube radius, even though the gap in the tube caused a finite density beyond this radius. At 35 μsec the radial variation of the density is nearly a first-order Bessel function.

Afterglow quenching experiments were performed by passing a small current pulse, starting at 20-μsec delay with 10-μsec duration, through the plasma column. This current pulse raises the electron temperature, and thus reduces the collisional radiative recombination, process (1), as the overall rate is theoretically inversely dependent on the electron temperature to about the 4.5 power. The visible radiation, the densities of most excited states, and the rate of associative ionization, process (3), are all reduced during this heating pulse, while the rate of ambipolar diffusion is increased due to the increase in the electron pressure. Because of these changes in the various rates, it is also expected that the densities of the ions and metastable states will be modified immediately after the heating pulse as well. Systematic measurements were thus made during the heating pulse (at 25-μsec delay) and after the heating pulse (35-μsec delay).

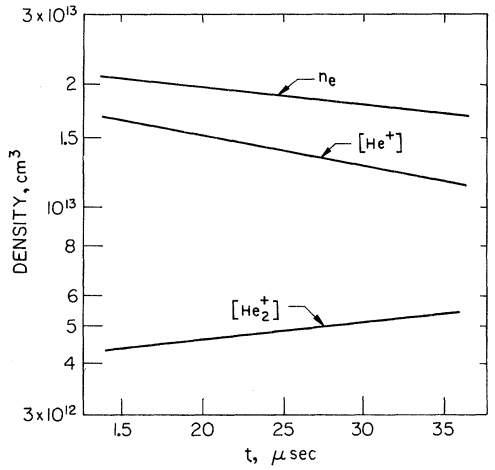

FIG. 4. Plot of the electron, atomic, and molecular ion densities on the axis of the plasma column versus the time after the end of the discharge pulse. These results are inferred from the spectroscopic measurements.

In Fig. 6 the change in intensities due to the heating pulse, both during and after the heating pulse, are shown for the λ3889 line originating from the He($3\,^3P$) atomic state and the λ4650 band originating from the $He_2(3p\,^3\Pi)$ molecular state. For small currents the intensities drop during the heating pulse and increase after the heating pulse. At currents above 200 mA, λ3889 begins to increase in intensity during the heating pulse, presumably due to the onset of excitation of the He($2\,^3S$) state, and both λ3889 and λ4650 decrease in intensity after the heating pulse, presumably due to the increased ambipolar diffusion. Similar results have been reported by Anderson,[64] and the technique has also been employed by Kenty[35] and Chen, Leiby, and Goldstein.[36]

The population densities of the higher-lying atomic levels during the heating pulse (25-μsec delay) and on the axis of the discharge are shown plotted in Fig. 7 as a function of the ionization energy. Since the electron density is not appreciably changed by the short heating pulse, straight lines representing equilibrium at a value of $(n_e n_i)^{1/2} = 1.67 \times 10^{13}$ cm^{-3} were fitted to the data, as shown,

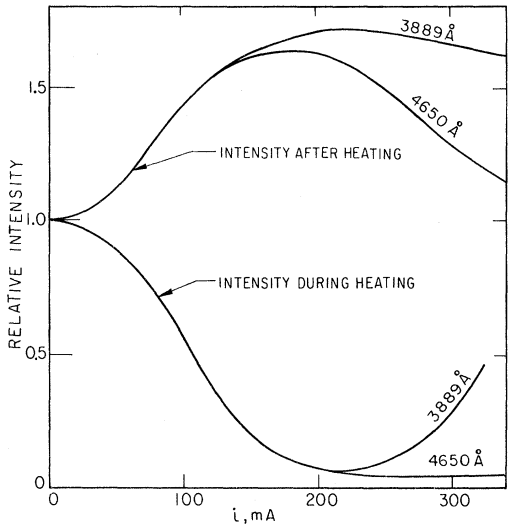

FIG. 6. Relative changes in intensity of an atomic ($\lambda = 3889$ Å) line and a molecular ($\lambda = 4650$ Å) band due to a short electron heating pulse, shown as a function of the pulse current.

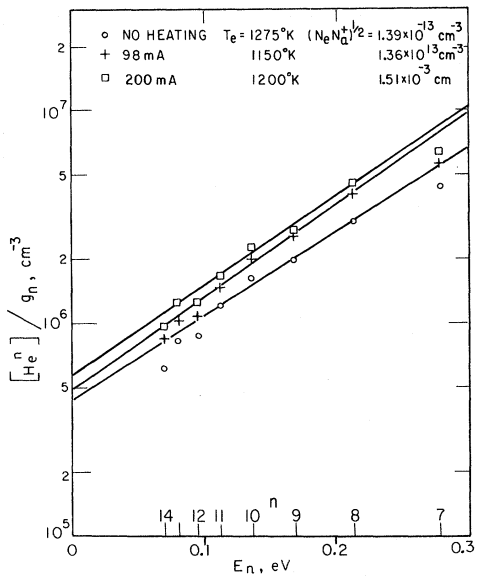

FIG. 8. Excited-state helium densities on the axis of the plasma column after the heating pulse (35-μsec delay) with pulse current as a parameter.

and the electron temperatures given on the figure were derived.

The quantum levels 10 to 13 show a systematic relative increase above equilibrium as the electron temperature is increased. It is believed that this is due to an overlapping of these levels by an N_2^+ impurity band. The N_2^+ impurity radiation was found to be independent of the electron temperature, and subtraction of a constant background intensity for the quantum levels 10 to 13 results in good agreement with the equilibrium line.

A similar analysis was made for a point 2 mm from the center of the plasma column, and although the electron temperature with no heating pulse was found to be the same, larger values were found with the heating pulse. In Table I these spectroscopically determined electron temperatures, at $r = 0$ and 2 mm, are given (at 25-μsec delay) along with the pulse current, electric field strength, and calculated electron temperatures to be described in Sec. IV C.

The population densities of the higher-lying atomic levels after the heating pulse (35-μsec delay), and on the axis of the discharge, are shown in Fig. 8 as a function of the ionization energy. Although the rise in density of these levels is quite marked, only rather imprecise changes in electron temperature and density can be found by attempting to fit straight lines to those levels expected to be in equilibrium with the free electrons. The values shown on the figure indicate a small, but uncertain, drop in electron temperature, accompanied by a small (~7%) rise in electron density.

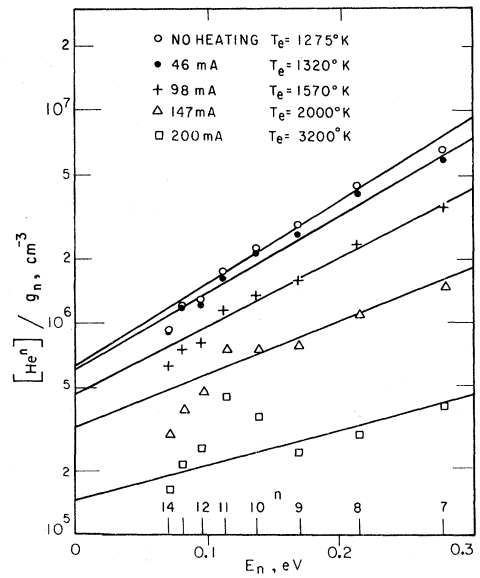

FIG. 7. Excited-state helium densities on the axis of the plasma column during the 10-μsec heating pulse (25-μsec delay), with pulse current as a parameter. The solid lines are fitted by assuming that the heating pulse does not change the electron density, and give the electron temperatures noted.

C. Plasma Conductance and Electron Temperature

The electrical conductivity was calculated according to the prescription given by Schweitzer and Mitchner,[65] with the electron-atom cross section taken from Frost and Phelps.[66] The radial variation of the conductivity was found using the spec-

troscopically determined values of n_e (Fig. 5) and T_e and then integrated over the column cross section to give the total plasma conductance. In Fig. 9 the calculated conductance is shown as a function of time, along with the values measured using the floating field probes with a small current pulse. Reasonable (~20%) agreement is found, although the calculated conductance does not decay as rapidly as the measurements indicate. This is probably due to errors in n_e and T_e near the wall of the tube, which were determined by extrapolation and are of lesser accuracy.

Figure 10 shows the calculated and measured conductances during the heating pulse plotted as a function of the heating pulse current. Reasonable agreement is found. Interestingly enough, the heating of the electrons introduces only a small change in the conductance. The conductivity associated with the electrons and neutrals (σ_{ea}) and the conductivity associated with the electrons and ions (σ_{ei}) are approximately equal at $T_e = 1275\ ^\circ\mathrm{K}$, while σ_{ei} is about eight times larger than σ_{ea} at $T_e = 4000\ ^\circ\mathrm{K}$. Since σ_{ea} decreases with increasing T_e, while σ_{ei} increases, it turns out that the total conductivity changes rather little.

In Fig. 11 comparison is made between the calculated and measured conductances after the heating pulse, as a function of the heating pulse current. Again, there is little dependence on the pulse current, and reasonable agreement is found.

The electron temperature is elevated above the gas temperature, in the absence of an electric field, because part of the energy available as a result of recombination goes into heating the electrons. Under the conditions of this experiment the dominant part of this heating should come from the electron deexcitation of the $He(2^3S)$ state, process (5) (see Sec. IV E for a discussion of the electron energy balance). This metastable electron heating will result in a power density H_0 which is approximately independent of the electron temperature (when the metastable density is constant). If the time rate of change of the electron temperature and the electron

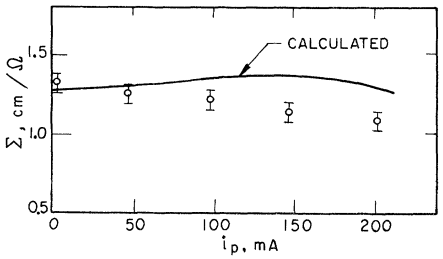

FIG. 10. Plot of the measured plasma conductance versus pulse heating current, during the heating pulse at 25-μsec delay, compared with that calculated using the spectroscopically measured values of electron density and temperature.

thermal conductivity are neglected, the electron energy equation can be written as

$$H_0 + iE = H_{ea} + H_{ei}\,, \tag{7}$$

where i is the current density, E the electric field strength, and H_{ea} and H_{ei} are the power loss rates due to elastic collisions of the electrons with atoms and ions, respectively. [See Bates and Kingston[5] for a discussion of Eq. (7) when iE is zero, and Robben[67] for the case where H_0 is zero.]

Since the lifetime of the $He(2^3S)$ state is long compared to the duration of the heating pulse, H_0 will be approximately constant during the heating pulse. Thus H_0 can be found from the measured n_e and T_e in the absence of a heating pulse, and then T_e can be calculated with a heating pulse using the measured total pulse current, the radial dependence of the conductivity, and the measured electric field strength. The resulting calculated values of T_e are given in Table I at $r = 0$ and 2 mm, where they can be compared with the spectroscopically determined temperatures. We see that the measured temperature difference between the center and the outer point is predicted by the theory, and is due to the electron-ion collisions. These collisions are much more important near the center, and they tend to

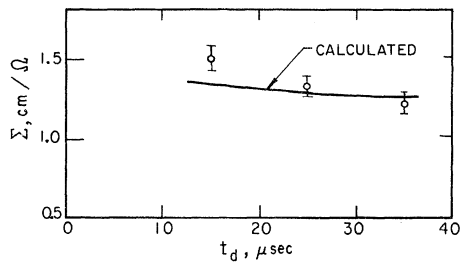

FIG. 9. Plot of the measured plasma conductance versus delay time, compared with that calculated using the spectroscopically measured values of electron density and temperature.

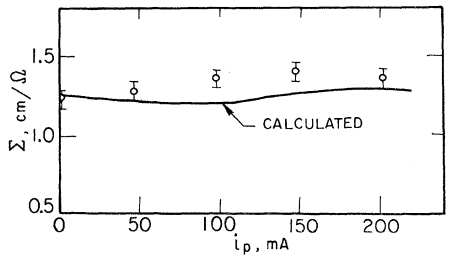

FIG. 11. Plot of the measured plasma conductance versus pulse heating current, after the heating pulse at 35-μsec delay, compared with that calculated using the spectroscopically measured values of electron density and temperature.

TABLE I. Comparison of the spectroscopically measured electron temperatures with those calculated from the measured electric field strength and current in the plasma column.

Electric field (V/m)	Center of discharge Measured electron temp.	Center of discharge Calculated electron temp.	2 mm from center Measured electron temp.	2 mm from center Calculated electron temp.
0	1275	1275	1275	1275
40	1320	1350	1350	1370
81	1570	1610	1650	1670
130	2000	2150	2220	2250
200	3250	3150	3800	3250

diminish i in Eq. (7) while increasing H_{ei}, resulting in a lowered electron temperature.

The effect of the thermal conductivity of the electrons was calculated and found to be relatively unimportant, at low electron temperatures because of the lack of an appreciable gradient, and at high temperatures because of the increased magnitude of the other terms in the energy equation. At the walls of the tube there is a loss of electron energy due to the diffusion of only higher-energy electrons through the sheath,[68] but this is small compared to the total electron energy loss in the plasma. Near the walls, though, the electron temperature will be considerably lower and dependent on the thermal conductivity. This lower electron temperature near the wall affects the accuracy of the calculated conductance of the plasma column.

The above comparisons of conductance and electron temperature establish a degree of confidence in the spectroscopic determinations of n_e and T_e. While these are not precision measurements in any sense, it is gratifying that the theoretical expressions for electron transport do lead to consistency with the experimental measurement.

The experimental data were also analyzed assuming a lower electron temperature (960 °K), so that the line indicating equilibrium in Fig. 2 passes through the levels with quantum numbers greater than 10. Then the calculated conductivity becomes smaller and the calculated electron temperature higher, leading to considerable disagreement with the measured values. The base electron temperature of 1275 °K leads to about the best over-all consistency between the various measurements and calculations.

D. Ionic Conservation

It is possible to make several checks on the conservation equations for the atomic and molecular ions, to see if agreement with the results calculated from processes (1)–(4) is achieved. Here we present the results of two such checks which do not make use of the afterglow quenching measurements. The rate of conversion of atomic to molecular ions appears to be in good agreement with known values of the processes, while the rate of electron recombination is found to be about one-half of the collisional radiative rate calculated by Bates, Kingston, and McWhirter,[1] in agreement with the previous measurements of Robben *et al.*[4] and the recent theoretical calculations of Mansbach and Keck.[69]

Using the values of n_e, $[He^+]$, and $[He_2^+]$ found at the center of the plasma column from the spectroscopic measurement, as shown in Fig. 3, the characteristic rates ν_e for the electrons, ν_a for the atomic ions, and ν_m for the molecular ions were found to be the following:

$$\begin{aligned} \nu_e &= -1.05\times10^4\ \text{sec}^{-1}\ , \\ \nu_a &= -1.70\times10^4\ \text{sec}^{-1}\ , \\ \nu_m &= \ \ 1.08\times10^4\ \text{sec}^{-1}\ . \end{aligned} \tag{8}$$

Also, the fraction of molecular ions at 25 μsec was found to be given by

$$[He_2^+]/n_e = 0.25\ . \tag{9}$$

Consider now the characteristic rate for the electrons. Process (1), collisional radiative recombination, is a loss process with a characteristic rate which we will denote by ν_{cr}. Process (4) reionizes some of these recombined ions, which rate we will denote by ν_{mm}. The combination of these two processes has been treated by Bates, Bell, and Kingston[52]; Stevefelt[70] has recently shown that process (4) is of more general importance in afterglow decay than previously recognized. Process (2), associative ionization, may also reionize recombined atomic ions; however, since many levels of the excited atom are involved, as proposed in the following paper, it appears that this process does not have much effect on the electron loss. Process (2) will then be neglected. We thus have

$$\nu_e = \nu_{cr} + \nu_{mm} + \nu_{ed}\ , \tag{10}$$

where ν_{ed} represents the electron ambipolar diffusion rate.

We will use the values of the ambipolar diffusion coefficients given in Ref. 8, 470 Torr cm^2 sec^{-1} for the atomic ion and 750 Torr cm^2 sec^{-1} for the molecular ion. To find the atomic ion diffusion rate ν_{ad} we will assume that the radial distribution of the ions follows the first-order Bessel function (which is approximately true, see Fig. 4), and taking into account the different gas and electron temperatures we obtain

$$\begin{aligned} \nu_{ad} &= -\frac{D_a}{\Lambda^2} \\ &= -\frac{D_a p_0}{\Lambda^2 p}\frac{T_g^{\,2}}{345\times273}\frac{1}{2}\left(1+\frac{T_e}{T_g}\right) \\ &= -7.0\times10^3\ \text{sec}^{-1}\ . \end{aligned} \tag{11}$$

In this formula Λ is the characteristic diffusion

length, T_g is the gas temperature, 345 °K was the gas temperature in the measurement of Ref. 8, and 273 °K is the reference temperature for the quoted value of $D_a p_0$. By a similar calculation we find the molecular diffusion rate ν_{md} to be

$$\nu_{md} = -1.1 \times 10^4 \text{ sec}^{-1} \quad . \tag{12}$$

The diffusion rate for the electrons is then given by the weighted average of (11) and (12). For process (4) we will use the rate constant $k_{mm} = 6.7 \times 10^{-10} \times T_g^{1/6}$ cm^3 sec^{-1} given in Ref. 52, and we find that

$$\nu_{mm} = k_{mm}[\text{He}(2\,^3S)]^2/n_e = 3.8 \times 10^3 \text{ sec}^{-1} \quad , \tag{13}$$

with $[\text{He}(2\,^3S)] = 6.0 \times 10^{12}$ cm^{-3} as determined by absorption measurements.[71] If we now solve Eq. (10) for ν_{cr}, we find the value given in the first row of Table II.

On the basis of the collisional radiative-recombination model the rate of recombination can be found by summing all radiative transitions to the principal-quantum-number-two states (plus a contribution from collisional transitions which is negligible in the present case), as was done by Robben, Kunkel, and Talbot.[4] Since we are assuming that the molecular ions follow the same model, the molecular radiation must be included as well. Absolute intensity measurements were only made of the $n\,^3\Sigma$-$2\,^3\Pi$ and $n\,'\Sigma$-$2\,'\Pi$ series; however, later measurements which included all measurable molecular bands, but at somewhat different discharge conditions, enable us to estimate the total molecular recombination rate. It is approximately 30% of the atomic rate, and thus is proportional to the molecular ion fraction as determined by the large quantum number intensity ratio. This gives additional evidence for the assumption that the recombination rate is the same for the molecular ions as for the atomic ions. The characteristic recombination rate derived from the radiated photon rate is given in the second row of Table II, and is seen to be about twice that found from the conservation equation.

The neglected rate of associative ionization may, according to the model proposed in the following paper, increase the rate of recombination above *a priori* calculations based on the collisional radiative model, but the rate calculated from the radiated photons should still be correct. Examination of the errors in the conservation equation calculation shows that if the electron temperature decreases by 7% during the period 15–35 μsec, which is slightly outside the estimated experimental error, an additional decrease of about 10% in n_e at 35 μsec as inferred from atomic line intensities would be found. This would increase ν_e by about 50%, which in turn would double the value of ν_{cr} in the first line of Table II and lead to agreement with the second line. Thus we believe the value in the second line of Table II represents the best measured value of ν_{cr}, although it depends on the assumption of some specific details of the recombination process.

TABLE II. Comparison of the characteristic rates for recombination.

	Rate (10^4 sec^{-1})
From conservation, Eq. (10)	−0.6
From radiated photon sum	−1.2
From tables of Bates, Kingston, and McWhirter (Ref. 1)	−2.7
From Mansbach and Keck (Ref. 69)	−1.3

The value of ν_{cr} in the third line of Table II was found from the tables of Bates, Kingston, and McWhirter[1] using the measured electron density and temperature. This value is somewhat more than twice that found from the photon sum.

Mansbach and Keck[69] have calculated low-energy classical electron excitation and ionization rates by a Monte Carlo trajectory technique, and find values considerably smaller than given by Gryzinski's[56] formulation for the excitation of highly excited atomic states. They use their results to calculate the collisional (neglecting radiation) recombination rate, and find the equation $\alpha = 2.0 \times 10^{-27}\, n_e [kT_e/e]^{-9/2}$ cm^3 sec^{-1}, where kT_e/e is the electron temperature in eV and n_e the electron density in cm^{-3}. The value of ν_{cr} derived from this formula is given in the last line of Table II, where it is seen to be in good agreement with the experimental value found from the photon sum.

The calculation of Mansbach and Keck[69] neglects the contribution of radiative transitions to the recombination rate, and thus is valid for high electron densities and low electron temperatures. The present plasma belongs to this class, as shown by calculation, and thus the result quoted in Table II does not require a significant radiative correction. The calculations of Bates, Kingston, and McWhirter,[1] based on Gryzinski's[56] cross sections, predicts approximately a factor of 2 larger rate for the present conditions. Less than 10% of this increase is due to radiative transitions, the remainder apparently being due to the use of larger cross sections. They also do not obtain a $T_e^{-9/2}$ behavior in the collisional limit.

In a more approximate treatment of collisional radiative recombination, Curry[17] uses a modified form of the Thomson collisional cross sections. He obtains a collisional recombination rate which is exactly one-half of that obtained by Mansbach and Keck.[69]

The summary of experimental measurements given by Curry,[17] and to a lesser extent the summary in Mansbach and Keck,[69] favor the results of Mansbach and Keck over any of the other theories.

Further, both the collisional deexcitation rates and the recombination rates found by Robben, Kunkel, and Talbot[4] are in good agreement with Mansbach and Keck's rates. Finally, the recent work of Johnson and Hinnov[16] led to collisional rates smaller than Gryzinski's,[56] which are in good agreement with the results of Mansbach and Keck. The conclusion is that Mansbach and Keck treat collisional recombination more correctly than Bates, Kingston, and McWhirter, and that radiative corrections should be added to their calculations in order to extend them to a wider range of plasma conditions.

Let us now consider the characteristic rate for conversion of atomic ions into molecular ions. The conservation equation for atomic ions is given by

$$\nu_a = \nu_{cr} + \nu_{ad} + \nu_{mm} - \nu_{a3b} - \nu_{aai} \ , \tag{14}$$

where ν_{a3b} is the characteristic rate of three-body molecular ion formation, process (3), referred to the atomic ion density, and ν_{aai} is the characteristic rate of associative ionization, process (2), referred to the atomic ion density. The conservation equation for molecular ions is given by

$$\nu_m = \nu_{cr} + \nu_{md} + \nu_{m3b} + \nu_{mai} \ , \tag{15}$$

where ν_{m3b} and ν_{mai} are now referred to the molecular ion density. We have assumed that ν_{cr} is the same for both ions, and further that associative ionization creates molecular ions from highly excited atomic states which have not recombined by process (1), as discussed in the following paper.

By subtracting Eq. (15) from Eq. (14), ν_{cr} will drop out. The rate of three-body conversion was taken from Oskam and Mittelstadt,[61] and converted to the gas temperature of 450 °K by assuming a $1/T$ variation.[48] The result is given by

$$\nu_{a3b} = -3 \times 10^3 \text{ sec}^{-1} \ . \tag{16}$$

The rate of associative ionization is determined in the following paper,

$$\nu_{mai} = 18 \times 10^3 \text{ sec}^{-1} \ . \tag{17}$$

From the measured atomic and molecular rates, relations (8), we find that $\nu_a - \nu_m = -28 \times 10^3$ sec^{-1}, while using the values of the various processes in the difference of the right-hand sides of Eqs. (14) and (15) leads to $\nu_a - \nu_m = -28 \times 10^3$ sec^{-1}. This perfect agreement is accidental, as our estimated error is of the order of 20%. Nevertheless, our treatment of the process of associative ionization, the dominant term in the formation of the molecular helium ions, seems to be correct. Further, this result is insensitive to small variations in electron temperature, unlike the result for electron conservation.

E. Conservation of Energy for Electrons

In this section known processes are used in the electron energy equation to see if agreement is obtained with the measured electron temperature of 1275 °K at 25-μsec delay. Since the He(2^3S) state plays an important role in the electron energy equation, the conservation equation for this state is also considered. We find a significant lack of agreement which is unexplained.

The electron energy equation is simplified by neglecting heat conduction, diffusion cooling, and the time rate of change of the electron energy. What remains then is simply a series of terms, representing the various processes which transfer energy to and from the electrons, that sums to zero. These terms, which are discussed in the following, are given numerically in Table III.

The electron energy loss H_0 in elastic collisions with ions and neutrals has been considered in Sec. IV C, and the value as determined by Eq. (7) is given in Table III in units of eV cm^{-3} sec^{-1}. It is interesting to note that this value indicates an energy loss per recombined electron of 29 eV, based on the recombination rate -2.2×10^{17} cm^{-3} sec^{-1} as determined by the emitted photon rate (see Table II). Since only 24.6 eV of energy are available for each recombined ion, at a maximum, this indicates that there must be an additional source of energy, such as the He(2^3S) state.

Direct electron deexcitation of the He(2^3S) state, process (5), results in the term H_{em} listed in Table III. A metastable density of 6×10^{12} cm^{-3} was used, with the rate constant taken from Bates, Bell, and Kingston.[52] If the inverse reaction is taken into account according to the model proposed by Ingraham and Brown,[60] a rate reduction of about 50% is found.

The rate of metastable ionizing collisions, process (4), has been given by Eq. (13). This process liberates 15 eV of energy, which has been used in calculating H_{mm} in Table III. Ingraham and Brown[60] have reasoned that only 9 eV will be transferred to the electron, on the average, with the rest being shared between the atom and ion. This is a complex problem, and it is not obvious that the logic of Ingra-

TABLE III. Magnitude of terms in the electron energy equation.

		Energy rate (10^{18} eV cm^{-3} sec^{-1})
H_0,	elastic collisions, Eq. (7)	6.2
H_{em},	electron deexcitation of metastable, process (5)	2.8
H_{mm},	ionizing metastable collisions, process (4)	1.1
H_{cr},	direct recombination, process (1)	0.2
H_{mol},	estimated for molecular ions	1.0

ham and Brown is correct.

With every recombination event the energy from the ionization limit down to the excited state where deexcitation proceeds by radiation is transferred to the free electrons. Byron, Stabler, and Bortz[2] discuss this problem and give a graph from which the value can be estimated. For our conditions about 1 eV is transferred, and this results in the value for H_{cr} in Table III.

Absorption measurements of the molecular metastable state $He_2(2\,^3\Sigma)$ gives a density of about 1×10^{12} cm^{-3}, which is too low to be an important independent energy source. If we thus assume that all molecular recombination events immediately result in a transfer of the metastable energy to the electrons, we find the value H_{mol} in Table III. It may well be, however, that an appreciable fraction of this energy is instead transferred to the atoms, since the molecule must eventually dissociate.

The sum of the sources in Table III is 5.1×10^{18} eV cm^{-3} sec^{-1}, about 85% of H_0 and within the estimated experimental error. This would be considered satisfactory agreement except that the time behavior of $He(2\,^3S)$ is not correctly predicted, as shown in the following.

Let us consider the characteristic rates for the $He(2\,^3S)$ state. These are summarized in Table IV, with process (4) and process (5) as losses, and with the atomic recombination rate given by the measured photon rate as a source. Thus we should have a net rate $\nu_{met}=-2.2\times10^4$ sec^{-1}, which would give about 35% reduction in the metastable density over the period 15–35 μsec. However, the nearly constant electron temperature indicates that ν_{met} is numerically less than 4×10^3 sec^{-1}. Further, when the electrons are heated in the 10-μsec pulse, essentially stopping the recombination rate, we should expect an additional 25% reduction in the metastable density after the heating pulse. This should lead to a reduction of the electron temperature to 1070 °K at 35 μsec, which is not supported by the data shown in Fig. 8.

There thus appears to be a discrepancy between the predicted rate for the $He(2\,^3S)$ metastable state and the rate inferred from the behavior of the electron temperature. Absorption measurements confirm that the density of the metastable state is nearly constant during this time, but on the other hand were not made with sufficient care to be highly reliable in this instance. However, we have not been able to find a reasonable explanation, and considering the possible combined errors in the electron temperature, absorption, and the rates entering into Table IV, it appears that the discrepancy is not too serious.

TABLE IV. $He(2\,^3S)$ characteristic rates.

Process	Rate (10^4 sec^{-1})
Electron deexcitation, process (5)	−2.4
Ionizing metastable collisions, process (4)	−2.3
Diffusion, D/Λ^2	−0.3
Formation by recombination	2.8

F. Dependence of Recombination Rate on Electron Temperature

As mentioned in Sec. IV D, the rate of recombination can, according to the collisional radiative model, be found by summing all radiative and collisional transitions to the principal-quantum-number-two level.[4] Since collisional transitions to this level are negligible, the intensity of the stronger lines will be approximately proportional to the recombination rate. In Fig. 12 the logarithms of the intensity of a number of the stronger atomic and molecular transitions are plotted as a function of the logarithm of the electron temperature, during the heating pulse at 25-μsec delay. The electron temperatures used are the "spectroscopic" electron temperatures given on Fig. 7. It is apparent that all lines and bands show the same dependence on T_e, within the experimental error, and we find an average slope, excluding the highest temperature, of −3.9. Assuming that other processes are not important under these conditions, this implies that the collisional radiative-recombination rate is proportional to $T_e^{-3.9}$ in the temperature range 1200–2000 °K. It also appears that the recombination rate does not follow a simple power law at temperatures as high as 3250 °K.

For comparison, the theory of Mansbach and Keck[69] predicts $\alpha\sim T_e^{-4.5}$ in the collisional limit (where radiative effects are neglected), a commonly assumed dependence in agreement with the earlier results of Hinnov and Hirschberg.[3] However, the calculations of Bates, Kingston, and McWhirter[1] predict $\alpha\sim T_e^{-5}$ in the collisional limit, but with inclusion of radiative effects give values of the exponent ranging from −4.5 at $T_e=1500$ °K to −3.7 at $T_e=3000$ °K, for $n_e=10^{13}$ cm^{-3}. This inclusion of radiation increases the recombination rate, especially at higher electron temperatures. If we assume that the Mansbach and Keck[69] collisional calculations are correct, and take the change in the exponent due to inclusion of radiative effects from the calculations of Bates, Kingston, and McWhirter,[1] then the experimental relation $\alpha\sim T_e^{-3.9}$ derived from Fig. 12 seems quite reasonable.

The data shown in Fig. 12 also tend to confirm the idea that recombination, insofar as it populates levels with principal quantum number 3 and larger, is a similar process for atomic and molecular helium ions. It might be expected that the associative ionization model proposed in the following paper would affect the similarity of atomic and molecular transitions shown in Fig. 12, but it probably pro-

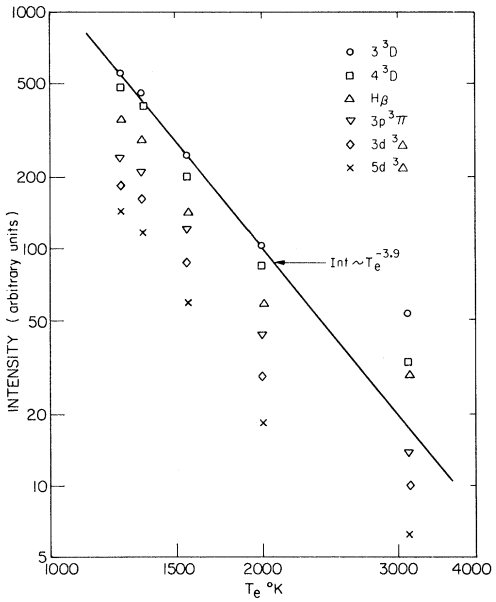

FIG. 12. Plot of the logarithms of the intensities of several atomic lines and molecular bands as a function of electron temperature.

duces only a small perturbation which is lost in the experimental error. We conclude from this section that radiative effects on the recombination rate cannot be neglected for most interesting recombining plasmas, and thus in order for the recombination model of Mansbach and Keck[69] to be generally useful an adequate treatment of radiation should be included.

V. SUMMARY AND CONCLUSIONS

The early afterglow of a short 1.3-A discharge in helium at 11 Torr was studied in some detail. Spectroscopic measurements of the number densities of excited atomic and molecular helium states were used to obtain the respective ion densities and electron temperature. The measured conductance of the plasma column was in good agreement with that calculated from the measured ion density. A small current pulse was used to selectively heat the electrons in the afterglow, and the resulting electron temperature as calculated from the electric field and current was in reasonable agreement with the spectroscopically measured electron temperature.

The rate of decay of electron density was about one-half of that obtained from the emitted photon rate, and about one-quarter of that found from the tables of Bates, Kingston, and McWhirter.[1] The recombination rate obtained from the emitted photon rate was in reasonable agreement with some previous measurements at lower pressures, and with the recent theoretical calculations of Mansbach and Keck.[69] A short review indicates that these latter calculations are in good agreement with a number of experimental measurements, and are probably more accurate than the calculations of Bates, Kingston, and McWhirter.[1]

The rate of conversion of atomic into molecular ions was dominated by associative ionization of excited atomic states, as reported in the following paper. Good agreement was obtained by including this process with other known processes. Finally, the dependence of the emitted photon rate on the electron temperature was found to be proportional to $T_e^{-3.9}$, somewhat smaller than given by the theory of collisional radiative recombination.

ACKNOWLEDGMENTS

We are indebted to Professor S. Lundquist and Dr. J. Braun for their interest in, and support of, this experiment. Thanks are due to Dr. K. Nygaard and Dr. E. Larsson for stimulating discussions, and to B. Fjällstom, who designed and constructed all of the electronic equipment. Finally, G. Abrahamsson, J. Johansson, and H. Stövne are acknowledged for their kind assistance. One of us (F. R.) acknowledges the support of the Air Force Office of Scientific Research and the National Science Foundation during completion of the analysis and writing of the manuscript at the University of California.

APPENDIX: HELIUM MOLECULAR-STATE OSCILLATOR STRENGTHS

The number density of an excited molecular level can be obtained from the intensity of a band originating from this level if the oscillator strength of the band is known. Since we were not able to find any information on the oscillator strengths for helium molecular bands in the literature, we used the Coulomb approximation as tabulated by Bates and Damgaard[63] to find the oscillator strengths of $2\,^1\Sigma - 3\,^1\Pi$ band and the $2\,^3\Sigma - n\,^3\Pi$ bands, $3 \leq n \leq 12$.

No mention is made in the Bates and Damgaard paper on the applicability of the Coulomb approxima-

TABLE V. Molecular helium band oscillator strengths.

Band	σ^2 (a.u.)	S (a.u.)	gf
$2s\,^3\Sigma - 3p\,^3\Pi$	0.91	5.46	0.36
$2s\,^3\Sigma - 4p\,^3\Pi$	0.27	1.62	0.13
$2s\,^3\Sigma - 5p\,^3\Pi$	0.109	0.96	0.088
$2s\,^3\Sigma - 6p\,^3\Pi$	0.056	0.34	0.032
$2s\,^3\Sigma - 7p\,^3\Pi$	0.035	0.21	0.020
$2s\,^3\Sigma - 8p\,^3\Pi$	0.020	0.12	0.012
$2s\,^3\Sigma - 9p\,^3\Pi$	0.013	0.080	0.0080
$2s\,^3\Sigma - 10p\,^3\Pi$	0.010	0.059	0.0059
$2s\,^3\Sigma - 11p\,^3\Pi$	0.0072	0.043	0.0043
$2s\,^3\Sigma - 12p\,^3\Pi$	0.0056	0.034	0.0034
$2s\,^1\Sigma - 3p\,^1\Pi$	1.23	2.46	0.15

tion to molecules; however, since these are Rydberg transitions, where the principal quantum number changes, the method should give good results. In fact, since the quantum defect of the molecular helium levels is so small (considerably less than in the case of atomic helium), the method might be even better than for the case of atomic helium.

The calculation is straightforward, and values for the factor σ^2, are given in Table V. The values for $n > 5$ are obtained by extrapolating σ^2 parallel to the value of σ^2 for the $2s$-np hydrogen series, as a function of n on semilogarithmic paper. This is intuitively reasonable, and previous experience with atomic helium,[4] where some variational calculations had been made for large n, showed it to be correct in that case. The factor σ^2 for the $2s\,^3\Sigma - 3p\,^3\Pi$ band is approximately 3.3 times larger than for the corresponding atomic multiplet, for larger n this ratio decreases to about 2.8. For the singlet band this ratio is 1.5.

The line strength S for the "multiplet" is obtained by multiplying σ^2 by $S(M)$, tabulated by Allen,[72] for example. The value for a $^1S - {}^1P$ transition is 3, but since in our case the p electron is only in the Π orbital, we used the value 2 for the $2s\,^1\Sigma - 3p\,^1\Pi$ band and 6 (instead of 9) for the $2s\,^3\Sigma - np\,^3\Pi$ bands. The resulting values of the line strength S and the product of the oscillator strength f and the multiplicity g are given in Table V.

The strength for one vibrational transition is obtained by multiplying the value in Table V by the vibrational overlap integral; this integral was taken to be approximately unity for the 0-0 vibrational transition as the internuclear separations of the two states are almost identical. The total intensity of the band is divided among the rotational transitions where the Hönl-London factors give the relative strength of each rotational transition. Due account must be taken of the fact that the helium molecule is homonuclear with nuclear spin zero, thus every alternate rotational line is missing.

From absolute intensity measurements of each rotational line in the $2s\,^1\Sigma$-$3p\,^1\Pi$, $2s\,^2\Sigma$-$3p\,^3\Pi$, and $2s\,^3\Sigma$-$4p\,^3\Pi$ bands, the total band intensity was found by analytically summing the best straight-line fit to a semilog plot of the number density of the upper level. Also, with considerably wider slits on the spectrometer so that the individual rotational lines were not resolved, the total integrated intensity of the band was obtained by scanning over the band. These two measurements were in good agreement (~20%). The intensities of the higher-principal-quantum-number members of the $2s\,^3\Sigma$-$np\,^3\Pi$ Rydberg series were found only by scanning over the band, as they were considerably weaker and the rotational structure was harder to measure accurately. The final results of all these measurements are shown in Fig. 2.

The densities of the higher n levels seem to lie on a line parallel to the atomic levels, at about one-third the density. However, the $3s\,^3\Sigma$ density is larger, and the $3s\,^1\Sigma$ lower, than would be expected if molecular helium behaved the same as atomic helium. In particular, all atomic levels with the same n seem to be maintained in thermal equilibrium at the electron temperature, while this is apparently not true for molecular helium. Three possibilities for this behavior have been considered. The electron collisional rates connecting these levels could be much smaller than for helium, but this seems unlikely since the electronic structure is so similar. There could be large three-body collisional rates,

$$He^n + 2He \rightarrow He_2^m + He \ ,$$

but the experiment of Teter and Robinson[54] makes this unlikely. Finally, the calculated oscillator strengths could be off, so that the result is spurious. We do not believe this to be so, but find it difficult to assess the possible errors.

---

*Present address: Service de Physique Atomique, Centre de Etudes Nucleaires de Saclay, BP No. 2, Gif-sur-Yvette, France.

†Work partially done at AB Atomenergi, Studsvik, Sweden.

[1]D. R. Bates, A. E. Kingston, and R. W. P. McWhirter, Proc. Roy. Soc. (London) A267, 297 (1962); A270, 155 (1962).

[2]S. Byron, R. C. Stabler, and P. I. Bortz, Phys. Rev. Letters 8, 376 (1962).

[3]E. Hinnov and J. G. Hirschberg, Phys. Rev. 125, 795 (1962).

[4]F. Robben, W. B. Kunkel, and L. Talbot, Phys. Rev. 132, 2363 (1963). There is a misprint in the table of helium oscillator strengths in this paper. The headings of the third and fifth columns should be interchanged, and the headings of the fourth and sixth columns should be interchanged.

[5]D. R. Bates and A. E. Kingston, Proc. Roy. Soc. (London) A279, 10 (1964); A279, 32 (1964).

[6]C. B. Collins and W. W. Robertson, J. Chem. Phys. 40, 2202 (1964).

[7]W. S. Cooper and W. B. Kunkel, Phys. Rev. 138, A1022 (1965).

[8]R. A. Gerber, G. F. Sauter, and H. J. Oskam, Physica 32, 2173 (1966).

[9]B. Stafford, J. Durham, and H. Schlüter, J. Chem. Phys. 45, 670 (1966).

[10]M. A. Gusinow, J. B. Gerardo, and J. T. Verdeyen, Phys. Rev. 149, 91 (1966).

[11]E. R. Mosburg, Phys. Rev. 152, 166 (1966).

[12]C. B. Collins and W. B. Hurt, Phys. Rev. 167, 166 (1968).

[13]S. von Goeler, R. W. Motley, and R. Ellis, Phys. Rev. 172, 162 (1968).

[14]A. A. Newton and M. C. Sexton, J. Phys. B 1, 669 (1968).

[15]G. K. Born and R. G. Buser, Phys. Rev. 181, 423

(1969).
[16]L. C. Johnson and E. Hinnov, Phys. Rev. 187, 143 (1969).
[17]B. P. Curry, Phys. Rev. A 1, 166 (1970).
[18]W. A. Rogers and M. A. Biondi, Phys. Rev. 134, A1215 (1964).
[19]E. E. Ferguson, F. C. Fehsenfeld, and A. L. Schmeltekopf, Phys. Rev. 138, A381 (1965).
[20]G. K. Born, Phys. Rev. 169, 155 (1968).
[21]C. B. Collins and W. B. Hurt, Phys. Rev. 177, 257 (1969).
[22]G. E. Veatch and H. J. Oskam, Phys. Rev. 184, 202 (1969).
[23]C. B. Collins, Phys. Rev. 177, 254 (1969).
[24]C. B. Collins and W. B. Hurt, Phys. Rev. 179, 203 (1969).
[25]J. P. Kaplafka, H. Merkelo, and L. Goldstein, Appl. Phys. Letters 15, 113 (1969).
[26]J. Berlande, M. Cheret, R. Deloche, A. Gonfalone, and C. Manus, Phys. Rev. A 1, 887 (1970).
[27]C. B. Collins, H. S. Hicks, and W. E. Wells, Phys. Rev. A 2, 797 (1970).
[28]M. A. Gusinow, R. A. Gerber, and J. B. Gerardo, Phys. Rev. Letters 25, 1248 (1970).
[29]J. Braun and K. Nygaard, in *Electricity from MHD* (International Atomic Energy Agency, Vienna, 1966), Vol. I, p. 557.
[30]J. Stevefelt and J. Johansson, Aktiebolaget Atomenergi, Stockholm, Report No. AE-418, 1971 (unpublished).
[31]H. Zinko, J. Stevefelt, and J. Johansson, in the Proceedings of the Fifth International Conference on Magnetohydrodynamic Power Generation, Munich, 1971 (unpublished).
[32]F. Robben and E. Hagberg, Aktiebolaget Atomenergi, Stockholm, Report No. TPM-FFA-762, 1967 (unpublished).
[33]J. Braun, Plasma Phys. 9, 93 (1967).
[34]F. Robben, in Ref. 29, p. 489.
[35]C. Kenty, Phys. Rev. 32, 624 (1928).
[36]C. L. Chen, C. C. Leiby, and L. Goldstein, Phys. Rev. 121, 1391 (1961).
[37]K. Bockasten, J. Opt. Soc. Am. 50, 826 (1960).
[38]J. Stevefelt, Aktiebolaget Atomenergi, Stockholm, Report No. AE-211, 1968 (unpublished).
[39]R. S. Mulliken, Phys. Rev. 136, A962 (1964).
[40]D. R. Bates, Phys. Rev. 77, 718 (1950).
[41]F. L. Arnot and M. B. M'Ewen, Proc. Roy. Soc. (London) A171, 106 (1939).
[42]J. A. Hornbeck and J. P. Molnar, Phys. Rev. 84, 621 (1951).
[43]See Ref. 39 for a brief discussion of the dissociation energy of He_2^+.
[44]M. P. Teter, F. E. Niles, and W. W. Robertson, J. Chem. Phys. 44, 3018 (1966).
[45]A. V. Phelps and S. C. Brown, Phys. Rev. 86, 102 (1952).
[46]H. J. Oskam and V. R. Mittelstadt, Phys. Rev. 132, 1445 (1963).
[47]E. C. Beaty and P. L. Patterson, Phys. Rev. 137, A346 (1965).
[48]F. E. Niles and W. W. Robertson, J. Chem. Phys. 42, 3277 (1965). Gerber, Sauter, and Oskam (Ref. 8) have criticized the $1/T$ dependence found in this paper.
[49]M. A. Biondi, Phys. Rev. 88, 660 (1952).
[50]A. V. Phelps and J. P. Molnar, Phys. Rev. 89, 1202 (1953).
[51]W. B. Hurt, J. Chem. Phys. 45, 2713 (1966).
[52]D. R. Bates, K. L. Bell, and A. E. Kingston, Proc. Phys. Soc. (London) 91, 288 (1967).
[53]C. B. Collins, in *Proceedings of the Ninth Conference on Phenomena in Ionized Gases, Bucharest* (Editura Academiei Republicii Socialiste Romania, Bucharest, 1969), p. 51.
[54]M. P. Teter and W. W. Robertson, J. Chem. Phys. 45, 661 (1966).
[55]G. J. Schulz and R. E. Fox, Phys. Rev. 106, 1179 (1957).
[56]M. Gryzinski, Phys. Rev. 115, 374 (1959).
[57]M. Gryzinski, Phys. Rev. 138, A336 (1965).
[58]J. W. Poukey, J. B. Gerardo, and M. A. Gusinow, Phys. Rev. 179, 211 (1969).
[59]D. J. T. Morrison and M. R. H. Rudge, Proc. Roy. Soc. (London) 91, 565 (1967).
[60]J. C. Ingraham and S. C. Brown, Phys. Rev. 138, A1015 (1965).
[61]H. J. Oskam and V. R. Mittelstadt, Phys. Rev. 132, 1435 (1963).
[62]Note the discussion of this point in C. B. Collins, Phys. Rev. 175, 160 (1968).
[63]D. R. Bates and A. Damgaard, Phil. Trans. Roy. Soc. London A242, 101 (1949).
[64]J. M. Anderson, in *Proceedings of the Fifth Conference on Ionization Phenomena in Gases, Munich* (North-Holland, Amsterdam, 1962), Vol. I, p. 621.
[65]S. Schweitzer and M. Mitchner, AIAA J. 4, 1012 (1964).
[66]L. S. Frost and A. V. Phelps, Phys. Rev. 136, A1538 (1964).
[67]F. Robben, Phys. Fluids 12, 1945 (1969).
[68]A simple formulation of the boundary conditions on the electron energy equation at a surface is given in R. C. Tseng and L. Talbot, AIAA J. 9, 1365 (1971).
[69]P. Mansbach and J. Keck, Phys. Rev. 181, 275 (1969).
[70]J. Stevefelt, J. Phys. D 7, 899 (1971).
[71]These absorption measurements were performed in a modified apparatus by J. Johansson; however, the conditions were nearly unchanged from the earlier work except for an improvement in purity.
[72]C. W. Allen, *Astrophysical Quantities* (Athlone Press, London, 1955).